

# Monolithic Arrays of Grating-Surface-Emitting Diode Lasers and Quantum Well Modulators for Optical Communications

N. W. Carlson, G. A. Evans, S. K. Liew, C. J. Kaiser

David Sarnoff Research Center

CN-5300

Princeton, NJ 08543-5300

CONFIDENTIAL A 633

## ABSTRACT

The electro-optic switching properties of injection-coupled coherent two-dimensional grating-surface-emitting laser arrays with multiple gain sections and quantum well active layers are discussed and demonstrated. Within such an array of injection-coupled grating-surface-emitting lasers, a single gain section can be operated as intra-cavity saturable loss element that can modulate the output of the entire array. Experimental results demonstrate efficient sub-nanosecond switching of high-power grating-surface-emitting laser arrays by using only one gain section as an intra-cavity loss modulator.

(NASA-CR-186772) MONOLITHIC ARRAYS OF  
GRATING-SURFACE-EMITTING DIODE LASERS AND  
QUANTUM WELL MODULATORS FOR OPTICAL  
COMMUNICATIONS (David Sarnoff Research  
Center) 18 p

N90-25674

Unclas  
CSCL 20F 63/74 0292247

# Monolithic Arrays of Grating-Surface-Emitting Diode Lasers and Quantum Well Modulators for Optical Communications

N. W. Carlson, G. A. Evans, S. K. Liew, C. J. Kaiser

David Sarnoff Research Center

CN-5300

Princeton, NJ 08543-5300

Diode lasers are attractive for applications as transmitters in free-space optical communications systems.<sup>1</sup> Because of their small size and high efficiency, a significant reduction in the weight of the host satellite for the transmitter is realized. Since most diode lasers have large angular beam divergences ( $> 10^\circ$ ), large collimation telescopes are necessary to provide the appropriate system beam divergence. Therefore any reduction in the angular beam divergence of the laser transmitter will result in further weight reductions in the host satellite. In addition, a narrower divergence beam also reduces the possibilities of interference, jamming, or data interception. For this type of application, a diode laser transmitter must be developed that has a power output of 500 mW or more, produces a narrow-divergence diffraction-limited single lobed far field, operates in a single spectral mode, and maintains both a stable far-field pattern and spectral output at multi-GHz modulation rates. Single element diode lasers are limited to operating powers of about 100 mW. Therefore, suitable coherent diode laser arrays will have to be developed in order to increase power, and over the last decade this has been an active area of research.<sup>2</sup>

Coherent monolithic two-dimensional arrays of injection-coupled grating surface emitting (GSE) diode lasers represent a new technology that shows

great promise for generating the high-power narrow-divergence output beams that are necessary for applications in optical communications systems as well as a variety of other optical systems. Already GSE arrays have demonstrated output powers in excess of 1 W, far-field beam divergences of  $1^\circ \times 0.01^\circ$ , and spectral outputs narrower than  $0.25 \text{ \AA}$ .<sup>3-4</sup> In this paper, we report on the use of non-uniform current distributions to obtain sub-nanosecond electro-optic switching and electro-optic gain in the power current characteristics of an injection-coupled monolithic array of GSE diode lasers. Experimental results demonstrate that GSE laser arrays may be efficiently modulated at appropriate rates for digital communications applications.

Monolithic two-dimensional GSE diode laser arrays are a class of laser structures that consist of many electrically-isolated gain sections that are fabricated within a network of second order distributed Bragg reflector (DBR) passive waveguides. An example of a specific monolithic two-dimensional GSE array is shown in Fig. 1. This structure has electrically-isolated gain sections that consist of ten Y-coupled ridge-guided lasers along the lateral direction. Along the longitudinal direction, adjacent gain sections (groups of ten Y-coupled ridge-guided laser sections) are connected by second order distributed Bragg reflector (DBR) passive waveguide sections. These DBR sections function in a three-fold manner. The second grating order provides wavelength selective feedback (for wavelengths at or very near the Bragg condition) necessary to support laser oscillation. In first order, the grating couples light out normal to the wafer surface. The transmissivity of the DBR section must be sufficiently large that adjacent gain sections will be injection coupled. Such structures are monolithic, because the incorporation of the second order DBR sections into the structure makes it possible to fabricate lasers at the wafer level without having to form cleaved facets as is done in

conventional edge-emitting diode laser arrays. A graded-index separate confinement heterostructure single quantum well (GRINSCH-SQW) structure (nominal layer compositions and dimensions are given in Fig. 1) is common to both the active gain sections and the passive DBR waveguide sections.<sup>3,4</sup> The GRINSCH-SQW is the active layer for the gain sections and the guide layer for the passive DBR waveguide sections. Although the unpumped quantum well in the DBR sections represents a loss, the absorption losses of the quantum well saturate to low values ( $<10\text{cm}^{-1}$ ) at optical powers of several milliwatts.<sup>5</sup> The details of fabricating GSE arrays are given in refereneces 3 and 4.

Since monolithic GSE laser arrays contain multiple gain sections, it should be possible to modulate the output of an entire GSE array by selectively varying the drive current to a single gain section so that it acts as an intra-cavity loss element for the entire array. This technique, which is referred to as intracavity electroabsorption loss modulation, has been used to demonstrate Q-switching and bistable switching in edge-emitting diode laser arrays with quantum well structure active layers<sup>6</sup> as well as conventional double heterostructure lasers.<sup>7-9</sup> The use of quantum well active layers provide both a high differential gain and potentially large depth of loss modulation in the active sections of the GSE array. Both of these conditions are necessary for obtaining high speed switching and short output pulses.<sup>6</sup> By choosing the grating period of the DBR sections of a GSE array so that the operating wavelength is on the short wavelength side of the gain peak, the magnitude of the loss modulation and the differential gain can be maximized.<sup>10</sup>

The operating wavelength of a grating-surface-emitting laser array is determined by satisfying the Bragg condition for the grating in the DBR sections:  $\lambda_{\text{GSE}} = \Lambda n_e$ , where  $\lambda_{\text{GSE}}$  is the operating wavelength of the array,  $\Lambda$  is the grating period, and  $n_e$  is the effective index of the transverse spatial mode in the

DBR waveguide. Wavelengths within the reflectivity bandwidth (which usually corresponds to about a 5 Å bandwidth centered on  $\lambda_{\text{GSE}}$ ) of the DBR section will be retro-reflected back into the gain sections so that laser oscillation of a GSE laser array only occurs inside this small bandwidth centered on  $\lambda_{\text{GSE}}$ . Therefore, with a knowledge of the gain spectrum and DBR waveguide effective index it is possible to select a specific operating wavelength by appropriate choice of the grating period. An example of how the operating wavelength of a GSE laser array can be set to the short wavelength side of the peak of the gain spectrum is shown in Fig. 2. Here, the photoluminescence spectrum of the GRINSCH-single quantum well structure of a 2-dimensional GSE laser array is shown. The peak of the quantum well photoluminescence spectrum (which is about 8510 Å for the spectrum in Fig. 2) corresponds closely to the peak of the gain spectrum. Fabry-Perot lasers from this structure had an operating wavelength of 8570 Å. However, the grating period of 2584 Å resulted in an operating wavelength of 8480 Å, which is about 30 Å to the short wavelength side of the peak of the photoluminescence.

To investigate the switching properties of injection-coupled GSE laser arrays, devices were fabricated with grating periods such that the Bragg condition was satisfied for wavelengths that were shorter than the peak of the gain profile. In order to identify those arrays that could be switched by electro-absorption loss, the power versus current (PI) characteristics were measured when only the current to one gain section (usually at or near the middle of the array) was varied and the currents to all other gain sections were set at the same value. Figure 3 shows characteristic PI curves measurement for a such a GSE array. This particular array consisted of 9 injection-coupled gain sections. An abrupt turn-on of this array is observed over a significant part of the operating range.

No hysteresis effects were observed in any of the PI curves that showed the sharp turn-on. Such effects are usually seen in the PI curves of lasers that are switched by modulation of an intra-cavity saturable loss. However, the testing of the GSE arrays reported here was all done under pulsed operating conditions (50 ns pulse width 0.1-2% duty cycle). This was necessary, since the arrays had to be mounted p-side up in order use the light out-coupled by the grating. Such transient operating conditions might obscure any hysteresis effects that might otherwise occur. Nevertheless, the sharp transition did exhibit some bistable characteristics. When the current to the center gain section was tuned near the center of the steep part of the PI curve, the time-resolved output (as detected by a PIN diode with 20 ns rise time) was a superposition of two distinct pulse shapes (operating states) as shown in Fig.4. As the current to the center gain section was tuned through the transition to higher current values, the off-state pulse disappeared and only the on-state remained. Conversely, as the current was tuned through the transition to lower currents, the on-state pulse disappeared leaving only the off-state pulse. The observation of both output pulses in the narrow current range that corresponded to the transition could be an indication of bistability.

In the sharp turn-on region of the PI curve, an increase in the current to the center gain section by about 50 mA produced a change in the power output of the entire array as high as 400 mW. The array gain sections had a series resistance of about 10 Ohms so an increase of the electric power of about 25 mW into the array produced 400 mW of optical power. This corresponds to a differential gain of 12 dB in the conversion of electric power to optical power. and shows that a GSE array can be modulated efficiently by switching the drive current to only a small fraction of the array. This is an important consideration

for high-speed free-space communications systems, because it can reduce the rf power (and the size of the electronics package) needed to modulate the array.

In order to measure the switching speed between the on and off state of the array, the arrival time of the pulse to the center gain section was delayed with respect to the pulses to the other gain sections and the time-resolved light output was measured using a Si avalanche photodiode with a rise-time of about 200 ps. It was necessary to switch the array in this manner since this array could only be operated under low duty cycle pulsed conditions with about 50-100 ns long pulses. Fig. 5 shows the shape of the current pulse that was used to drive the gain section and the resulting time-resolved optical output pulse of the array (as measured with the avalanche photodiode). The pulse has a rise time of 420 ps and is just over 3 ns in duration. A longer fall time of about 1 ns is observed. This could possibly be due to heating of the array (p-side up operation) or the transient operating conditions.

The time-averaged far-field output and spectral output were measured when the array was operated to produce the optical pulse output that is shown in Fig. 5. These data are shown in Fig. 6. The time-averaged far-field output is predominantly a single-lobed in the longitudinal direction with an angular beam divergence which is  $0.05^\circ$  or less ( $0.03^\circ$  is resolution of this measurement). There is significant secondary lobe structure outside the dominant lobe. This is caused by wafer non-uniformities and surface roughness of the wafer, as discussed in reference 1. The spectral output (shown on a log intensity scale with 1 Å spectral resolution) is 2 Å wide at intensities 30 dB down in intensity from the peak wavelength with no other side modes observed outside this bandwidth. The measured spectral width is broader than the instrument resolution. Since this array was operated with short pulses (50-100 ns current pulses with no dc bias) to all gain sections and the spectrum was recorded by

averaging over many pulses, it is not too surprising that some spectral broadening was observed. While the current pulses are applied to the gain sections, the carrier density is always in a transient state. In steady-state operation where a dc bias would be applied to all gain sections, as shown in Fig. 7, the carrier density would be in a steady-state situation. A capacitively-coupled rf pulse applied to the center gain section (which is dc biased just below the transition as shown in Fig. 6) would switch the array on and off. In this mode of operation, the total carrier density of the array is always very close to the threshold value.<sup>11</sup> Therefore, electroabsorption loss modulation of a dc biased GSE array should exhibit considerably less spectral broadening because the fluctuations in the carrier density are lower than an array operated under transient conditions.

In conclusion, electro-optic switching and electro-optic gain accompanied by fast switching times have been demonstrated in two-dimensional GSE diode laser arrays. The PI curve characteristics and sub-nanosecond switching properties described above were only observed in GSE arrays operated at wavelengths that were on the short wavelength side of the of the peak of the gain spectrum. This is strong evidence that within a 2-dimensional GSE array, selected gain sections (with quantum well active layers) can be operated as intra-cavity saturable loss elements that efficiently modulate the output of the entire array at high frequencies. The use of multiple quantum well structures as the active/waveguide layers in GSE laser arrays should further improve the modulation and switching characteristics of these devices.<sup>6,10</sup> Along with the high power and low beam divergence output properties, these new results show that coherent GSE arrays have the capability to operate as high-speed transmitters in free-space optical communication systems. *not clear*



## References

- 1) J. D. Barry, "Design and system requirements imposed by the selection of GaAs/GaAlAs single mode laser diodes for free-space optical communications," IEEE J. Quantum Electron., vol. QE-20, pp.478-491,1984.
- 2) D. Botez and D. E. Ackley, IEEE Circuits and Devices vol. 2, pp.8-17 (1986) and references therein.
- 3) G. A. Evans, N. W. Carlson, J. M. Hammer, M. Lurie, J. K. Butler, S. L. Palfrey, R. Amantea, L. A. Carr, F. Z. Hawrylo, E. A. James, C. J. Kaiser, J. B. Kirk, W. F. Reichert, S. R. Chinn, J. R. Shealy, P. S. Zory, Appl. Phys. Lett. 53, pp.2123-2125 (1988).
- 4) G. A. Evans, N. W. Carlson, J. M. Hammer, M. Lurie, J. K. Butler, S. L. Palfrey, R. Amantea, L. A. Carr, F. Z. Hawrylo, E. A. James, C. J. Kaiser, J. B. Kirk, W. F. Reichert,, accepted for publication in IEEE J. Quantum Electron.
- 5) H. Okamoto, Jpn. J. Appl. Phys., vol.26, pp.315-330 (1987).
- 6) Y. Arakawa, A. Larson, J. Paslaski, A. Yariv, Appl. Phys. Lett., vol. 48, pp.561-563, (1986).
- 7) G. J. Lasher, Solid-State Electron., vol. 7, pp.707-716, (1964).
- 8) J. K. Carney, C. G. Fonstad, Appl. Phys. Lett., vol. 38, pp. 303-305, (1981).
- 9) H. Kawaguchi, IEE Proc. vol.141, pp.141-148, (1982).
- 10) K. Kojima, K. Kyuma, S. Noda, J. Ohta, K. Hamanaka, Appl. Phys. Lett., vol. 52, pp.942-944, (1988).
- 11) D. Z. Tsang, J. N. Walpole, IEEE J. Quantum Electron., vol. QE-19, pp. 145-156, (1983).

## Figure Captions

Figure 1: Schematic diagram of a 2-D injection-coupled GSE array with Y-coupled ridge-guided lasers in the lateral direction. The insets show the lateral waveguide structure, composition and thicknesses of the wafer structure, and schematic diagram of the distributed Bragg reflector waveguide sections.

Figure 2: The photoluminescence spectrum of the GRINSCH-single quantum well active/waveguide layer of a 2D-GSE laser array is shown.

Figure 3: Power versus current curves of a 9x10 GSE array that exhibits switching characteristics. The current to the center gain element is indicated on the horizontal axis and the total power output of the array is shown on the vertical axis. The set current values,  $I_b$  to the remaining gain sections are shown on the right next to each curve.

Figure 4: The time-resolved output of the array is shown with the array was operated in the middle of the steep transition part of the PI curve.

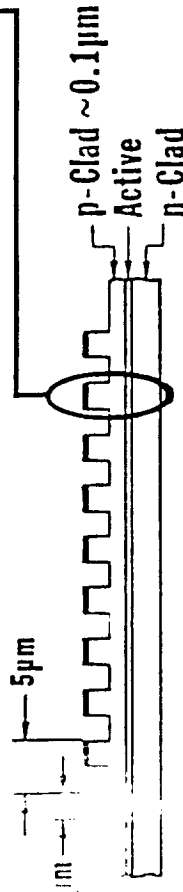
Figure 5: Both the current pulse and the resulting optical pulse output of the GSE array are shown. The optical pulse was detected with an avalanche photodiode which had a rise time of about 200 ps.

Figure 6: The time-averaged far-field and spectral outputs corresponding to the optical output pulse in Fig. 5 are shown.

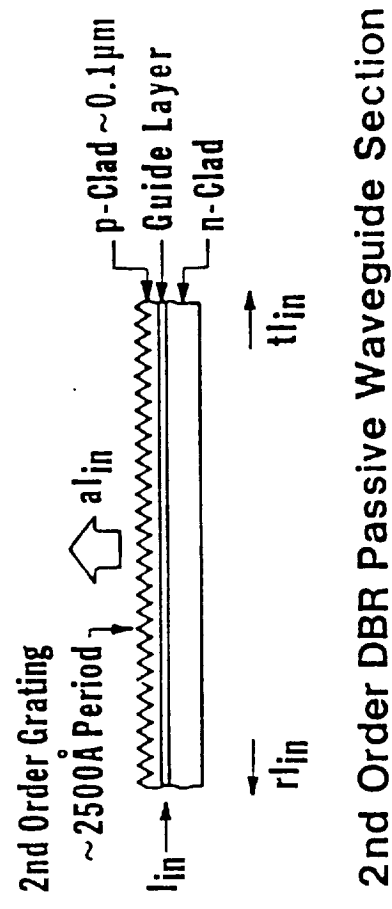
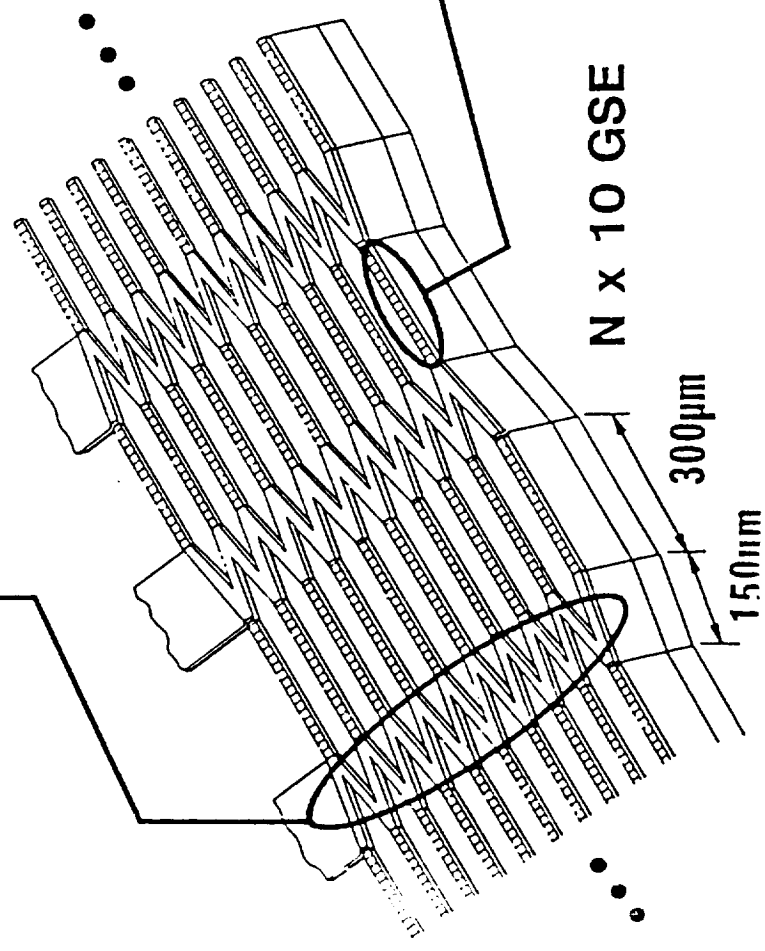
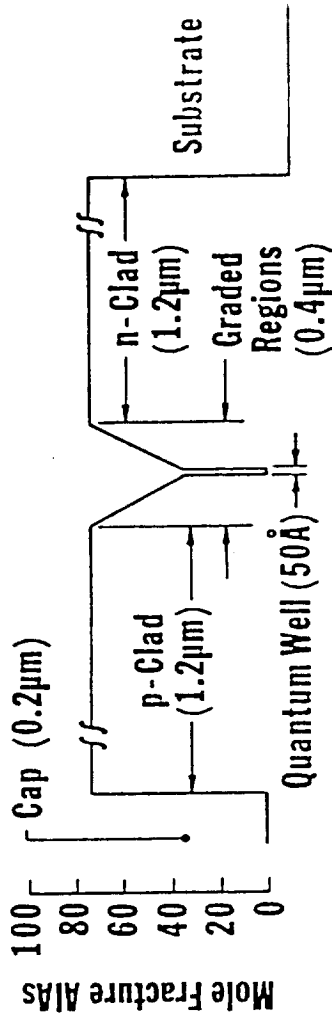
Figure 7: Schematic diagram of steady-state biasing of a GSE array for operation using intra-cavity electroabsorption loss modulation.

# of Injection-Coupled Gain Sections  
 # of Laterally-Coupled Lasers per Gain Section

Y-Ridge Guided Gain Section



GRIN SCH-SQW Active Layer



2nd Order DBR Passive Waveguide Section

FIGURE 1

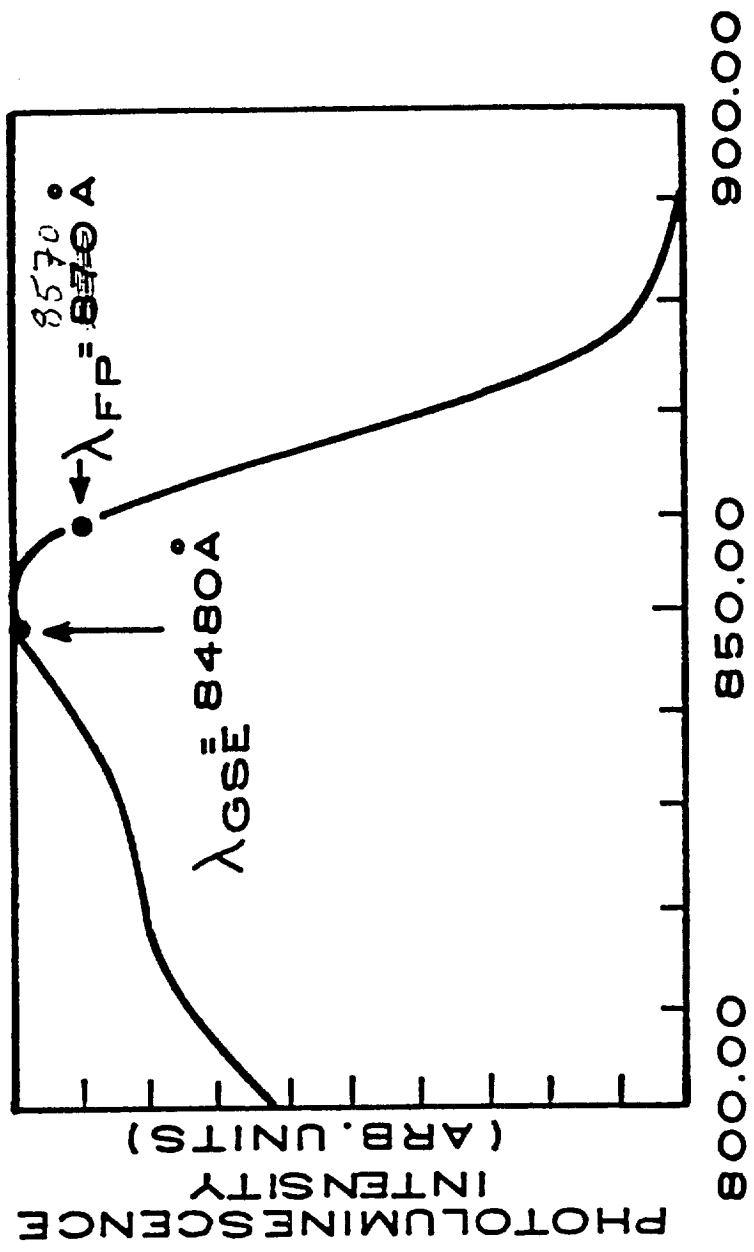


FIGURE 2

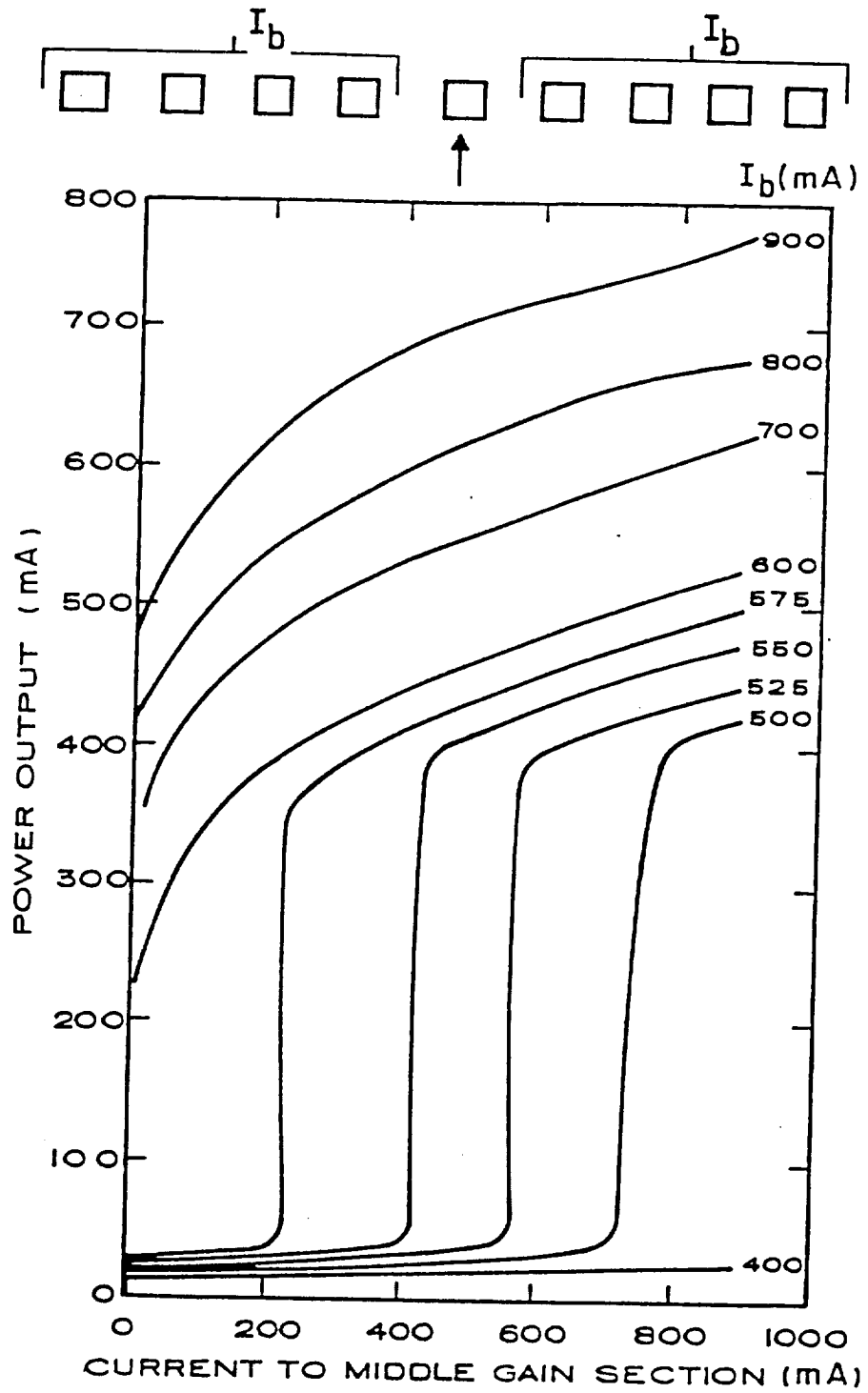


FIGURE 3.

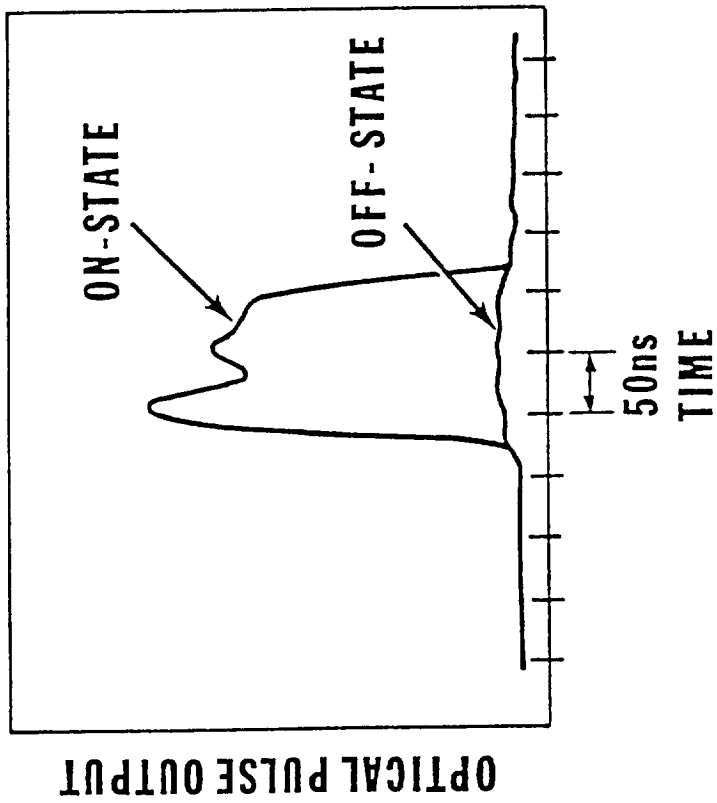
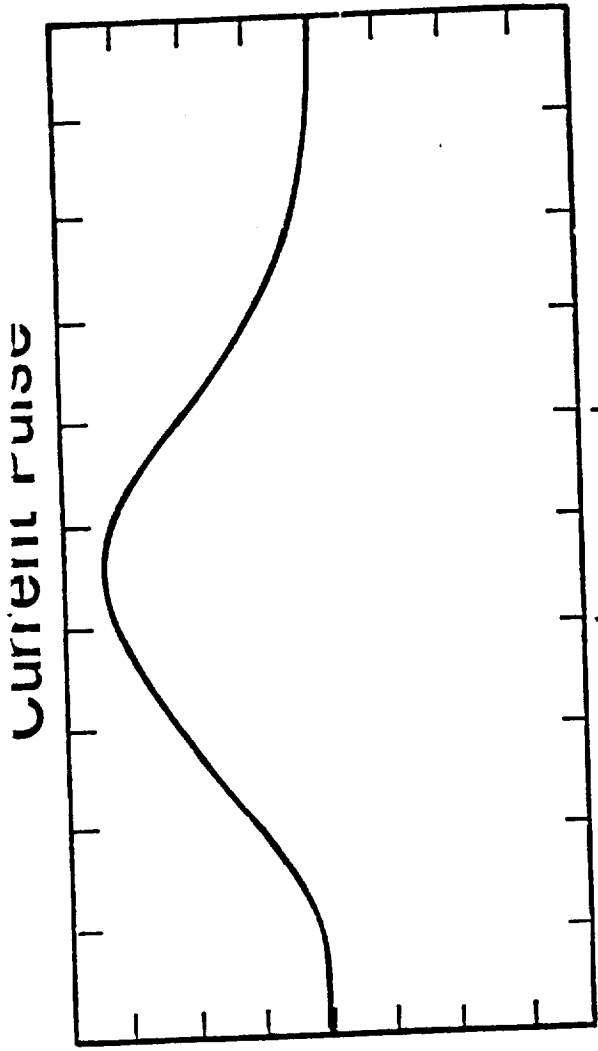
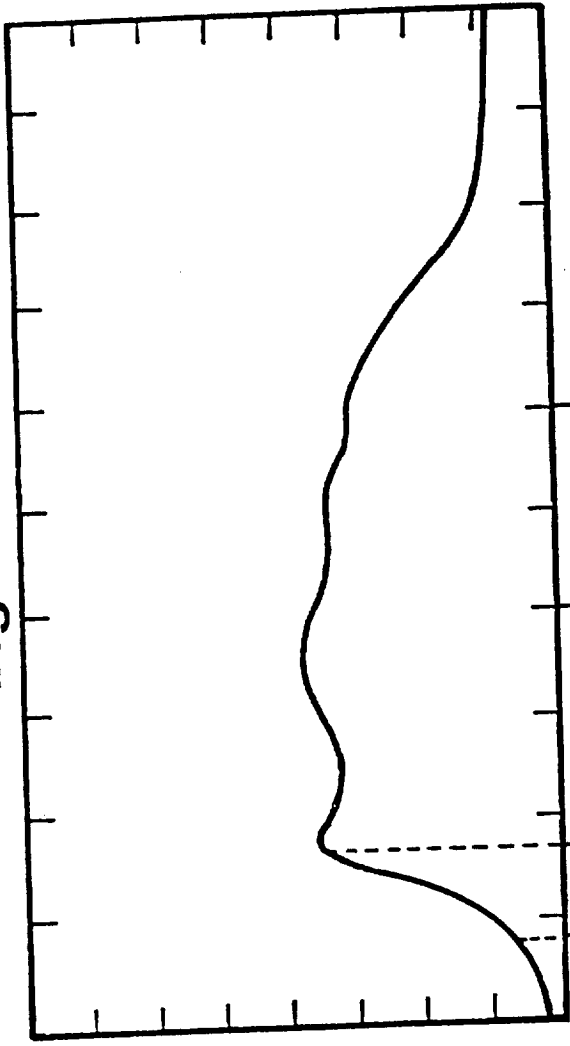


FIGURE 4



10ns

Light Pulse



1ns

420ps

ORIGINAL PAGE IS  
OF POOR QUALITY

FIGURE 5



ORIGINAL PAGE IS  
OF POOR QUALITY

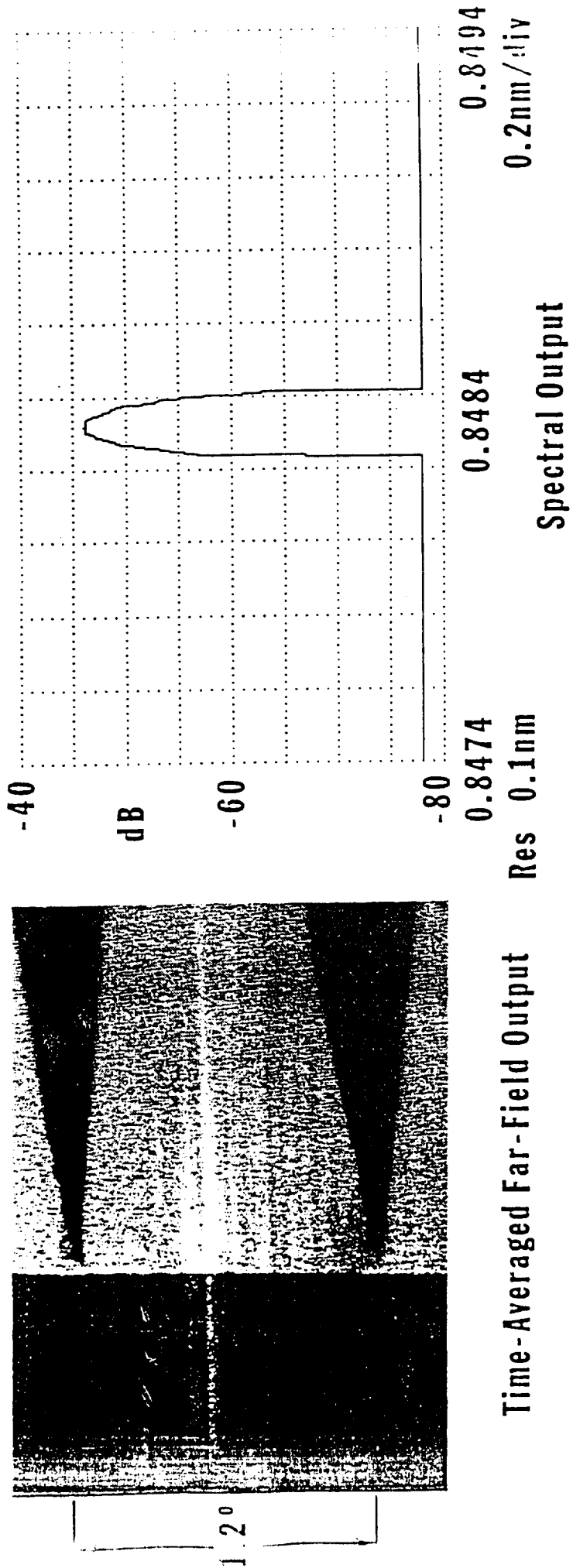
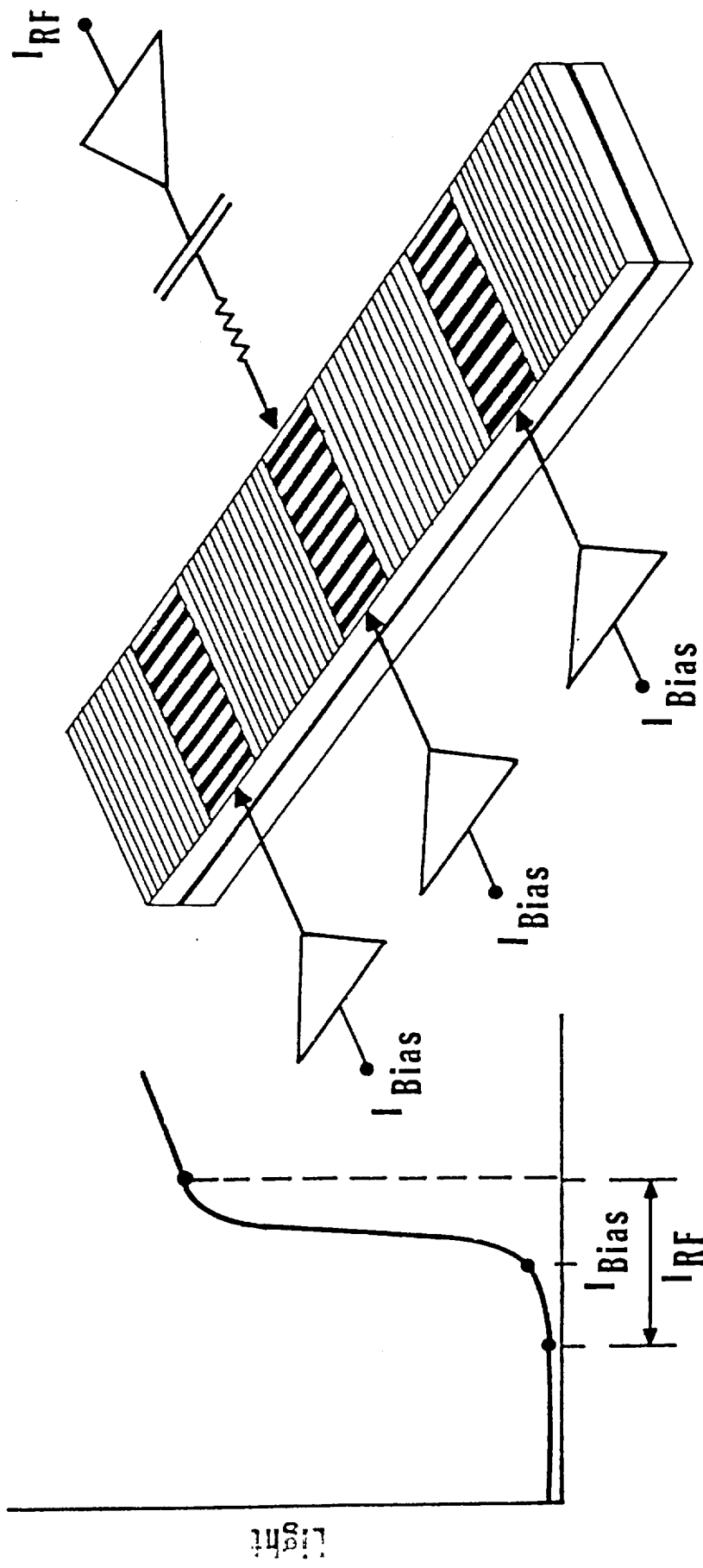


FIGURE 6



Current to Middle Gain Section